Proceedings of the 28th IEEE
EMBS Annual International Conference
New York City, USA, Aug 30-Sept 3, 2006

A Reconstruction Algorithm for Helical CT Imaging on PI-planes

Hongzhu Liang, Cishen Zhang and Ming Yan

***Abstract*— In this paper, a Feldkamp type approximate reconstruction algorithm is presented for helical cone-beam Computed Tomography. To effectively suppress artifacts due to large cone angle scanning, it is proposed to reconstruct the object pointwisely on unique customized tilted PI-planes which are close to the data collecting helices of the corresponding points. Such a reconstruction scheme can considerably suppress the artifacts in the cone-angle scanning. Computer simulations show that the proposed algorithm can provide improved imaging performance compared with the existing approximate cone-beam reconstruction algorithms.**

***Keywords*—Helical multislice CT, Feldkamp-type reconstruction, Half-scan CT**

I. Introduction

Helical multislice Computed Tomography (CT) has been developed for rapid and volumetric scanning with high axial image resolution for medical diagnosis. Algorithms for helical multislice CT reconstruction are classified into the approximate and the exact algorithms. While exact algorithms can produce high quality images, they require large amount of computation ([1]-[4]). Compared with exact algorithms, approximate algorithms can provide a feasible compromise between the image quality and computational efficiency [5]-[8] and, thus, have been popularly adopted.

Approximate reconstruction algorithms can be further grouped as 2-dimensional (2D) and 3-dimensional (3D) methods with respect to the input data dimension. While 2D methods are limited by the cone beam angle and helix pitch value, some non-transversal / non-planar reconstruction methods have been proposed [5], [6]. Among 3D reconstruction algorithms, Feldkamp (FDK) method is popularly adopted [7] due to its accuracy and computational efficiency. However, these algorithms have difficulties and suffer from artifacts at large cone angle scanning. Especially, the imaging performance at the rim region of interest (ROI) are considerably deteriorated, due to the large off-plane angle (the angle between the projection ray beam and the reconstruction plane). This directly limits the usage of large cone angle scanning and the scanning speed and efficiency.

In this paper, we propose an FDK-type algorithm to reconstruct transversal planar slice by computing each reconstruction point on a unique customized tilted plane. The selected tilted reconstruction plane passes through the PI-line of the corresponding reconstruction point and is close to the corresponding PI-helix segment. Thus it reduces the effective cone angle of the reconstruction point. While such a pointwise reconstruction requires extended projection data from half-scan projection, it does not involve considerably more online computational workload. It is shown that the proposed algorithm can provide improved imaging performance and image quality enabling large sized detector and large cone angle being applied for multislice CT imaging.

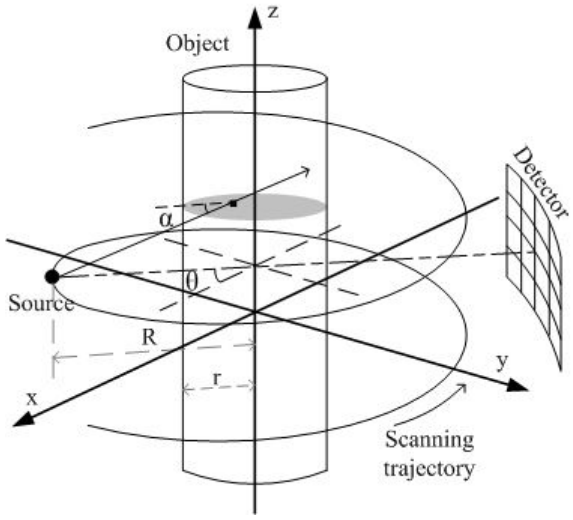

Fig. 1. Helical CT scanning geometry.

The rest of this paper is organized as follows. Section 2 presents the geometry of helical CT scanning and introduces the tilted plane for approximate reconstruction. Section 3 presents the proposed reconstruction algorithm, followed by computer simulation results and discussions. Section 4 is conclusion.

II. CT scanning and projection data formation

A. Helical scanning geometry

The geometry of the helical multislice CT scanning is shown in Fig.1 in a Cartesian coordinate system $x-y-z$. The X-ray source, denoted by S, moves around the z axis along a helical trajectory. Let R be the radius of the helix, r be the radius of objective cylindrical support, θ the source rotation angle, p be the pitch value of the helix, and w be the detector collimation width. Then the scanning translation speed in the z direction is $h = \frac{pw}{2\pi}$ and the position of the X-ray source can be represented as $(x_s, y_s, z_s)^T = (R\cos\theta, R\sin\theta, h\theta)^T$. For any point of the object, its off-plane angle, as shown in Fig. 1, is defined as the angle between the reconstruction plane and the ray-beam passing through this point at source rotation angle θ, and is denoted by α.

H. Liang and M. Yan are with School of Electrical & Electronic Engineering, Nanyang Technological University, 639798, Singapore lianghongzhu@pmail.ntu.edu.sg

C. Zhang is with School of Electrical & Electronic Engineering and School of Chemical & Biomedical Engineering, Nanyang Technological University, 639798, Singapore.

B. FDK off-plane reconstruction

It follows from FDK method that the reconstruction of a point (x, y, z) from cone beam half-scan projection data $D(\cdot)$

$$f(x,y,z) = \int_0^{\pi+2\sigma} \frac{D_w^f(m,n,\theta)d\theta}{U^2}, \tag{1}$$

where σ is the maximum fan-angle of cone-beam,

$$U = \frac{R + x\sin\theta - y\cos\theta}{R}, \tag{2}$$

$$D_w^f(m,n,\theta) = \frac{R}{\sqrt{R^2 + \frac{m^2}{\rho^2} + \frac{n^2}{\rho^2}}}[\omega(m,\theta)D(m,n,\theta)] * g(m). \tag{3}$$

is the filtered and weighted data set of $D(\cdot)$, (m, n) is the coordinates of the detector with m denoting the length of each detector row and n denoting the detector row number, $g(\cdot)$ is the 1D ramp filter, '$*$' denotes the convolution $\omega(\cdot)$ is conjugate weighting factor and ρ is the ratio of source-detector distance to source-center distance.

Alternatively, the cone-beam projection data can be re-bined into cone-parallel projection data set [9]. Therefore, the FDK reconstruction is as follows:

$$f(x,y,z) = \int_0^{\pi} \frac{1}{\sqrt{R^2 + \frac{s^2}{\rho^2}}} R[\omega'(\eta)D_p(t,s,\eta)] * g(t)d\eta, \tag{4}$$

where $D_p(\cdot)$ is the cone-parallel data set, (t, s) is the virtual cone-parallel detector in which t denotes the length of virtual detector row and s is the virtual detector row number, η is the source rotation angle of the rebinned cone-parallel data set, $\omega'(\cdot)$ is the conjugate weighting factor for cone-parallel projection data set. Since the conjugate data only exist at source rotation angle 0 and π, $w'(\cdot)$ equals to 0.5 at these two angle and equals to 1 otherwise [8].

With the above formulations, FDK reconstruction of off-plane ROI will produce cone-beam artifacts which depends on the off-plane angle of the objective points. To suppress these artifacts, it is essential to reduce the distance between the source and the reconstruction plane (i.e., source off-plane distance).

C. Tilted PI-plane for pointwise reconstruction

To reduce the off-plane distance of the object plane without affecting the object translation speed, we propose pointwise reconstruction on uniquely customized tilted planes. This tilted plane is essentially related to the properties of PI-line. Referring to Fig.2, we name an object point $\lambda(x_\lambda, y_\lambda, z_0)$ which is on an unique PI-line connecting two points $s_1(\theta_1)$ and $s_2(\theta_2)$ on the source helical trajectory while $0 < \theta_2 - \theta_1 < 2\pi$. The tilted reconstruction plane, denoted by Ω, is determined by the PI-line $\overrightarrow{s_1 s_2}$ connecting $s_1(\theta_1)$ and $s_2(\theta_2)$ and the center point s_3 of the PI-helix $\widehat{s_1 s_2}$ which is at the source rotation angle $\theta_3 = \frac{\theta_1+\theta_2}{2}$. Note that the plane Ω is of the family of κ-plane [4] and we denote it as PI-plane in this paper.

Since each point to be reconstructed has a unique PI-line, the PI-plane is a function of point λ, written as $\Omega(\lambda)$. The

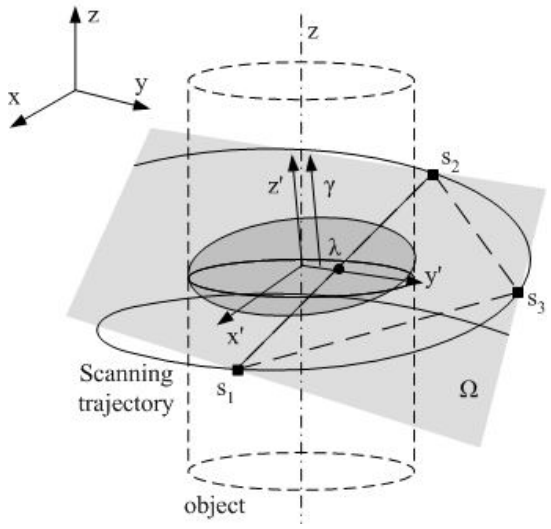

Fig. 2. The proposed PI-plane Ω and the tilted Cartesian coordinates $x' - y' - z'$.

normal vector of $\Omega(\lambda)$, $\vec{\gamma} = (a, b, c)^T$, satisfies the following equation.

$$\begin{bmatrix} R\cos\theta_1 & R\sin\theta_1 & h\theta_1 \\ R\cos\theta_2 & R\sin\theta_2 & h\theta_2 \\ R\cos\theta_3 & R\sin\theta_3 & h\theta_3 \end{bmatrix} \begin{bmatrix} a \\ b \\ c \end{bmatrix} = 0. \tag{5}$$

Note that $c \neq 0$ since $\vec{\gamma}$ in not on $x - y$ plane.

The PI-plane $\Omega(\lambda)$ defines a new Cartesian coordinate system $x' - y' - z'$ with z' being defined by the normal vector $\vec{\gamma} = (a, b, c)^T$ and the $x' - y'$ plane being defined by the PI-plane. Specifically, the transformation between the coordinate systems $x - y - z$ and $x' - y' - z'$ is given by

$$[\,x' \quad y' \quad z'\,]^T = T_2 T_1\,[\,x \quad y \quad z\,]^T, \tag{6}$$

where

$$T_1 = \begin{bmatrix} 1 & 0 & 0 \\ 0 & \cos\beta_1 & \sin\beta_1 \\ 0 & -\sin\beta_1 & \cos\beta_1 \end{bmatrix},\ T_2 = \begin{bmatrix} \cos\beta_2 & 0 & \sin\beta_2 \\ 0 & 1 & 0 \\ -\sin\beta_2 & 0 & \cos\beta_2 \end{bmatrix} \tag{7}$$

and

$$\beta_1 = -\arctan\frac{c}{b},\ \beta_2 = \arctan\frac{a}{\sqrt{b^2 + c^2}}. \tag{8}$$

The source $S(x_s, y_s, z_s)$ in the new coordinate system is

$$[x'_s \quad y'_s \quad z'_s]^T = T_2 T_1 [x_s \quad y_s \quad z_s]^T, \tag{9}$$

The off-plane angle of the point λ at source rotation angle θ with respect to PI-plane $\Omega(\lambda)$ is given as follows

$$\alpha = \arcsin\Big(\frac{d(\theta)}{\sqrt{(x_s - x_\lambda)^2 + (y_s - y_\lambda)^2 + (z_s - z_0)^2}}\Big), \tag{10}$$

where $d(\theta)$ is the source off-plane distance to the PI-plane $\Omega(\lambda)$ given as,

$$\begin{aligned} d(\theta) \quad = \quad & \frac{1}{\sqrt{a^2 + b^2 + c^2}}\big[(ax_s + by_s + cz_0) \\ & -(aR\cos\theta_1 + bR\sin\theta_1 + ch\theta_1)\big]. \end{aligned} \tag{11}$$

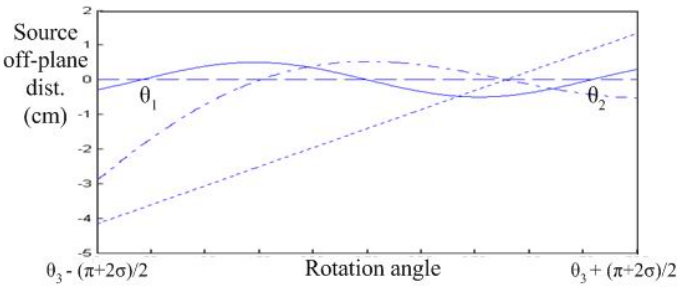

Fig. 3. The comparison of source off-plane distance to different reconstruction planes. The solid curve denotes the off-plane distance of PI-plane at each source angle, while the dash-dot curve denotes the off-plane distance of the ASSR tilting plane, and the dot curve is of the off-plane distance of the objective transversal plane.

It satisfies $d(\theta) > 0$ if the source is at the same side of the PI-plane and $d(\theta) < 0$ if it is at the opposite side. The off-plane distance of the source to the PI-plane is much less than that between the source and the objective transversal plane. Thus the reconstruction of the PI-plane is subject to considerably less effective cone angle than that of the conventional transversal plane.

To show the reduced effective cone angle, we simulate a scanning helix with parameters [$R = 50$cm, $h = 5$cm/π]. An object point is chosen arbitrarily and its PI-line is found. While the source moves along the half-scanning helix which is extended from the centre point of the PI-helix, the source off-plane distance to the corresponding PI-plane is recorded, as shown in Fig.3. For comparison, the off-plane distances to the transversal objective plane and the ASSR tilted reconstruction plane [5] are also calculated respectively.

III. Reconstruction and Simulation

A. Reconstruction on the tilted plane

We propose the following steps of the proposed FDK-type reconstruction of the objective point $\lambda(x_\lambda, y_\lambda, z_0)$ on the tilted PI-plane $\Omega(\lambda)$.

1. Collect the cone-beam projection data set D, and rebin the whole data set to obtain a cone-parallel data set [9]. The rebinning from the original data set D to the cone-parallel data set D_p is as follows

$$D_p(t, s, \eta) = D\Big(\frac{tR}{\sqrt{R^2 - t^2}}, s, \eta + \arcsin\frac{t}{R}\Big). \qquad (12)$$

2. Filter the cone-parallel data D_p row-wisely. Note that this filtering is tangential to the original data set D due to the parallel rebinning. Denote the filtered data set as Q.

3. Calculate the PI-plane and the reconstruction data range:

(3-a) Determine the PI-line $\overrightarrow{s_1 s_2}$ on which the point λ locates.

(3-b) Determine the normal vector $\vec{\gamma} = (a, b, c)^T$ of the PI-plane $\Omega(\lambda)$, following from (5).

(3-c) Build the new Cartesian system $x'-y'-z'$ and obtain the source position in the new coordinate system following (9).

4. A half-scan data set ranging at $[\theta_3 - \frac{\pi+2\sigma}{2}, \theta_3 + \frac{\pi+2\sigma}{2}]$ ($\theta_3 = \frac{\theta_1+\theta_2}{2}$) is selected from the filtered data set Q.

5. Extract the data required for reconstructing the point λ as in the following:

$$Q_\lambda(\eta) = Q\Big(\frac{Rt_\lambda}{R - s_\lambda}, \frac{R(z_0 - h\eta - h\arcsin\frac{t_\lambda}{R})}{R - s_\lambda}, \eta\Big), \qquad (13)$$

$$t_\lambda = x_\lambda\cos\eta + y_\lambda\sin\eta,\ \ s_\lambda = -x_\lambda\sin\eta + y_\lambda\cos\eta.$$

(t_λ, s_λ) is the point λ coordinates in the rotating coordinates (rotating with the source). Then multiply the data Q_λ with new cone-beam weighting factors calculated in the $x'-y'-z'$ coordinate system and with respect to the PI-plane $\Omega(\lambda)$. Refer to (4) the cone-beam weighting is

$$\bar{Q}_\lambda(\eta) = \frac{R'}{\sqrt{R'^2 + \frac{s'^2}{\rho^2}}}\, Q_\lambda(\eta), \qquad (14)$$

where R' and s' are respectively the source rotating radius and the detector row number calculated in the $x' - y' - z'$ coordinate system,

$$R' = \sqrt{x_s'^2 + y_s'^2}\ ,\ \ s' = \frac{d\big(\eta + \arcsin\frac{t_\lambda}{R}\big)}{R' - s_\lambda} d_{sd} \qquad (15)$$

with the off-plane distance $d(\cdot)$ being calculated following (11).

6. Referring to (4), implement the backprojection to obtain the value of point λ, as follows:

$$f(\lambda) = \int_{\eta_{\min}}^{\eta_{\max}} \omega'(\eta)\ \bar{Q}_\lambda(\eta) d\eta, \qquad (16)$$

$$\eta_{\min} = \theta_3 - \frac{\pi + 2\sigma}{2} - \arcsin\frac{t}{R},\ \ \eta_{\max} = \eta_{\min} + \pi.$$

B. Computer simulation

In this section, the proposed algorithm is tested with phantom models at simulated helical CT scanning, compared with ASSR 2D-rebinning reconstruction [5] and conventional FDK transversal reconstruction [7]. The simulated helical scanning system is defined as $R = 600$mm, source–detector distance $d_{sd} = 1000$mm, $p = 0.5$. There are 500 projections per rotation. The source collimator is adjusted to fit different sized detectors (16-row, 32-row and 64-row).

A $256 \times 256 \times 256$mm low-contrast Clock Phantom is adopted for simulation. The 16-row and 32-row detectors are simulated for different cone-angle scanning. Fig.4 shows the simulated imaging results. It is shown that the proposed algorithm can effectively suppress the cone-beam artifacts compared with the results of other two methods, especially for the large cone-angle reconstruction.

A $256 \times 256 \times 256$mm Dish phantom is adopted for numerical comparisons. The phantom has a 1mm thick grey dish (grey value=0.9) with two co-axial bright circles (grey value=1.0). The ambient has grey value 0. The dish is reconstructed with different algorithms at large cone-angle (64-row detector). The reconstructed values on the central line are displayed and compared, as shown in Fig.5. It is shown that the proposed algorithm can achieve more accurate reconstruction in the rim area.

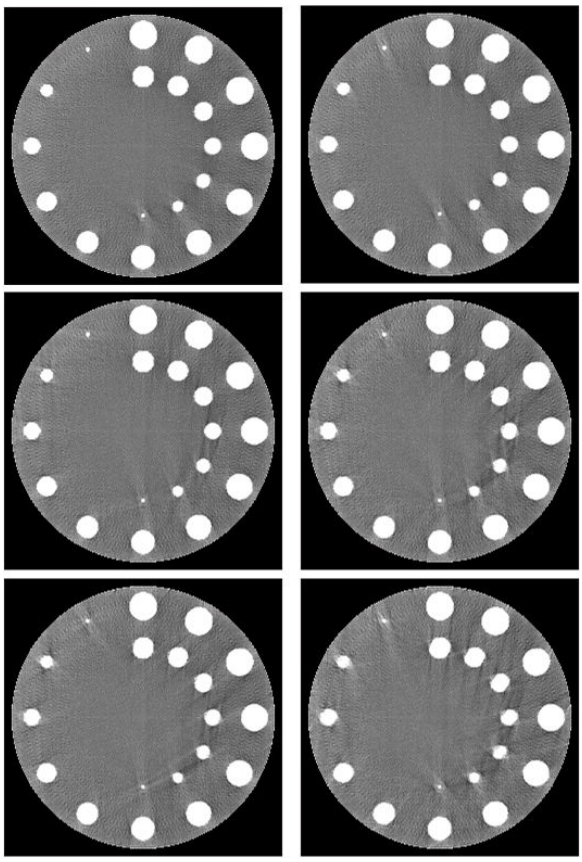

Fig. 4. Computer simulation imaging results. From the top are, respectively, the results of the proposed algorithm, ASSR and the conventional FDK. Images in the left column are with the small cone-angle (16-row detector) and that in the right column are with the large cone-angle (32-row detector).

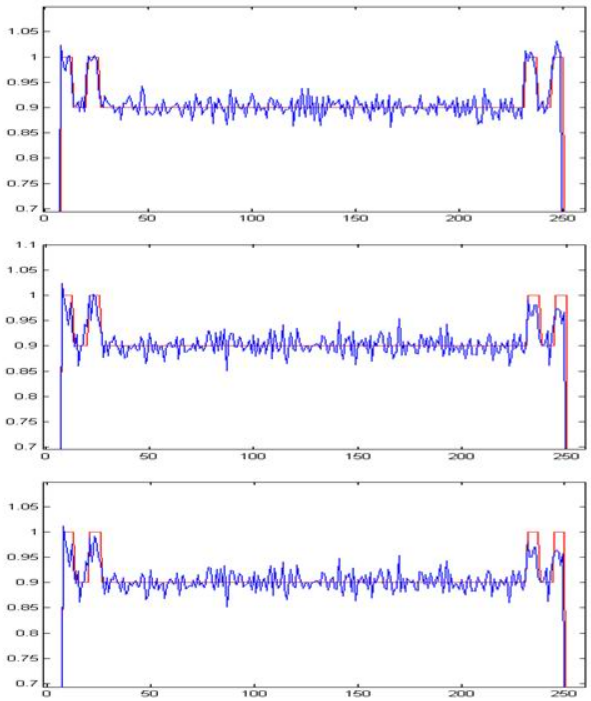

Fig. 5. Numerical results of large cone-angle (64-row detector) reconstruction. The straight lines denote the original values. From the top are, respectively, the results with the proposed algorithm, ASSR and the conventional FDK.

C. Discussion

Compared with the conventional FDK reconstruction, the new proposed algorithm needs additional computation to form the PI-planes and the tilted coordinate systems. Fortunately these additional calculations (step 3) do not involve use of the projection data. Therefore they can be precalculated and stored before scanning. Based on the new coordinate system, the additional workload including the source's new coordinates calculation (9) and the new cone-weighting factor calculation (15) can also be calculated off line. Moreover, due to the cone-parallel rebinning, the whole projection data set needs to be filtered only once before the reconstruction. Therefore, the on-line workload of the proposed algorithm is minimized and it does not cost much more time and space than the conventional FDK method does.

IV. Conclusions

This paper presents an FDK-type approximate reconstruction algorithm for helical multislice CT system. For constructing a transversal slice with less cone-beam artifacts, we propose pointwise reconstruction on a customized unique tilted PI-plane which passes through the PI-line of the reconstruction point. Compared with the existing algorithms, the proposed algorithm can effectively suppress cone-beam artifacts in the large cone-angle scanning without large additional online computation.

References

[1] A. Katsevich, "An improved exact filtered backprojection algorithm for spiral computed tomography," Advances in Applied Mathematics, Vol.32, pp. 681-697 (2004).

[2] Y. Zou and X. Pan, "Exact image reconstruction on PI-lines from minimum data in helical cone beam CT," Phys. Med. Biol., Vol. 49, pp. 941-959 (2004).

[3] Y. Zou and X. Pan, "Image reconstruction on PI-lines by use of filtered backprojection in helical cone-beam CT," Phys. Med. Biol., Vol. 49, pp. 2717-2731 (2004).

[4] F. Noo *et al.*, "Exact helical reconstruction using native cone-beam geometries," Phys. Med. Biol., Vol. 48, pp. 3787-3818 (2003)

[5] M. Kachelriess, S. Schaller and W. Kalender, "Advanced single-slice rebinning in cone-beam spiral CT," Med. Phys., Vol. 27, pp. 754-772 (2000).

[6] L. Chen, Y. Liang, D. J. Heuscher, "General surface reconstruction for cone-beam multislice spiral computed tomography," Med. Phys., Vol. 30, pp. 2804-2821 (2003).

[7] L. A. Feldkamp *et al.*, "Practical cone-beam algorithm," J. Opt. Soc. Am., Vol. 6, pp. 612C9 (1984).

[8] H. Hu. Multi-slice helical CT: Scan and reconstruction. Medical Physics, 26(1), pp. 5-18 (1999).

[9] X. Tang, *et. al.*, "A three-dimensional-weighted cone beam filtered backprojection (CB-FBP) algorithm for image reconstruction in volumetric CT helical scanning", Phys. Med. Biol., Vol. 51, pp. 855-874 (2006).